

Superhard diamondlike BC₅: A first-principles investigation

Chao Jiang,^{1,*†} Zhijun Lin,^{2,*‡} and Yusheng Zhao^{2,*§}

¹Structure/Property Relations Group (MST-8), Los Alamos National Laboratory, Los Alamos, New Mexico 87545, USA

²LANSCE–Lujan Neutron Scattering Center, Los Alamos National Laboratory, Los Alamos, New Mexico 87545, USA

(Received 31 July 2009; revised manuscript received 9 October 2009; published 4 November 2009)

We perform first-principles density-functional calculations to identify the possible crystal structure of a superhard diamondlike BC₅ phase, which was recently synthesized under high-pressure and high-temperature conditions. Interestingly, we find only a small total-energy difference between the energetically most favorable ordered configuration and the fully disordered state of BC₅ modeled using a 54-atom special quasirandom structure, indicating a weak ordering tendency. It is thus likely that the BC₅ phase synthesized under experimental conditions is disordered in nature. Such a conclusion is further corroborated by the fact that the disordered BC₅ structure displays volume-per-atom, bulk modulus and its pressure derivative, and simulated x-ray diffraction spectrum in good agreements with experiments.

DOI: 10.1103/PhysRevB.80.184101

PACS number(s): 61.50.Ah

Diamond is known as the hardest material with exceptional bulk modulus (442 GPa) and shear modulus (535 GPa).¹ However, applications of diamond are limited by its poor resistance to oxidation as well as reaction with ferrous metals. Due to the increasing demand of superhard materials ($H_v > 40$ GPa), great efforts have been made to search for superhard materials with better thermal and chemical stabilities than pure diamond. Superhard BC₂N and BC₄N compounds were synthesized at high pressures and high temperatures.^{2,3} In recent years, materials in the B-C system have also attracted increasing interest. Solozhenko *et al.*⁴ prepared a composite using graphitelike BC₃ as a starting material. The composite exhibited extreme hardness (88 GPa). Very recently, Solozhenko *et al.*⁵ reported the high-pressure temperature synthesis of a cubic diamondlike phase with a stoichiometry of BC₅, the highest boron content known to date. This structure exhibits extremely high Vickers hardness and fracture toughness, and is ~ 500 K more thermally stable than pure diamond. Theoretically, Calandra and Mauri⁶ demonstrated that BC₅ is superconducting with a critical temperature of the same order as that of MgB₂. During the review process of the present paper, two interesting papers on this BC₅ compound also appeared.^{7,8} Yao *et al.* predicted a thermodynamically stable $I\bar{4}m2$ phase. Another candidate structure with $P\bar{1}$ symmetry, whose x-ray diffraction (XRD) pattern fits well with the experimental one, was also obtained.⁷ The mechanical and electronic properties of diamondlike BC_x phases were also studied by Liang *et al.*⁸

Due to the similar and small atomic masses of boron and carbon, it is challenging to determine the exact atomic arrangement of diamondlike BC₅ from experimental XRD patterns. Such structural information is, however, crucial for a fundamental understanding of its intrinsic physical and mechanical properties. In this paper, we report a systematic search for the possible crystal structure of diamondlike BC₅ using first-principles calculations based on density-functional theory. Our calculations are performed using the all-electron projector augmented wave method within the generalized gradient approximation (GGA) of Perdew, Burke, and Ernzerhof,⁹ as implemented in Vienna *ab initio* simulation package (VASP).¹⁰ Our previous study¹¹ demonstrates that

GGA gives structural properties of γ -B₂₈ in excellent agreement with experiments. The electronic wave functions are expanded using a plane-wave basis set with a large cutoff energy of 500 eV. The k -point meshes for Brillouin-zone sampling are constructed using the Monkhorst-Pack scheme¹² and the total number of k points times the total number of atoms per unit cell is at least 10 000 for all structures. Our convergence tests show that these parameters guarantee high numerical accuracy for both total-energy and stress calculations, which is essential in view of the small energy differences between the different lattice configurations of BC₅ considered in our study. By computing the quantum-mechanical forces and stress tensor, the lattice constants and internal atomic positions of all structures are fully relaxed using a conjugate-gradient scheme.

In order to resolve the crystal structure of BC₅, we first redefine the crystal structure of cubic diamond (with $Fd\bar{3}m$ space group) to a hexagonal lattice by the following transformation of lattice vectors

$$\begin{pmatrix} 1 & 0 & 0 \\ 0 & 1 & 0 \\ 0 & 0 & 1 \end{pmatrix} \rightarrow \begin{pmatrix} 0 & -0.5 & 0.5 \\ 0.5 & 0 & -0.5 \\ 2 & 2 & 2 \end{pmatrix}. \quad (1)$$

A 12-atom hexagonal supercell with an ideal c/a ratio of $2\sqrt{6}$ is constructed. Through replacing two of the 12 carbon atoms with boron, we obtained a total of nine possible symmetrically inequivalent structures. Note that structure BC₅-1 [Fig. 1(a)] is the same as the structure adopted by Calandra and Mauri.⁶ All the rest eight configurations (BC₅-2 to BC₅-9) are shown in Figs. 1(b)–1(i), respectively. The calculated crystal structural parameters for BC₅-1 are in excellent agreement with those reported by Calandra and Mauri,⁶ which suggests the reliability of present calculations. Table I shows the energetics and equilibrium volumes of the fully relaxed BC₅- m ($m=1-9$) structures. Here the formation energy of a diamondlike B_xC_{1-x} structure is defined as follows:

$$\Delta E = E(B_xC_{1-x}) - xE(B) - (1-x)E(C), \quad (2)$$

where $E(B)$ and $E(C)$ are the first-principles calculated total energies (per atom) of pure boron and carbon, both in the

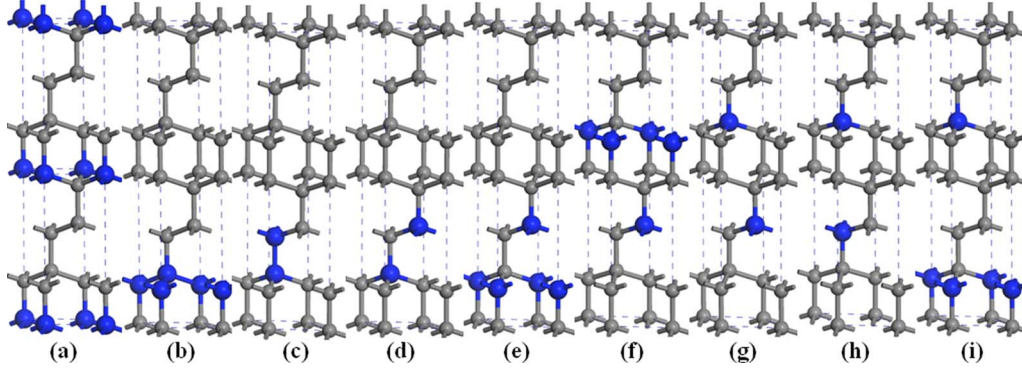


FIG. 1. (Color online) Crystal structures of BC_5-m ($m=1-9$) derived from the diamond lattice according to Eq. (1). The darker and lighter spheres are boron and carbon atoms, respectively. The structure in (a) is the same as that adopted in Ref. 6.

diamond structure. $E(B_xC_{1-x})$ is the total energy of diamond-like B_xC_{1-x} . For BC_5 , $x=1/6$. Note that, here we restrict our discussions to the possible arrangement of boron and carbon atoms on an underlying diamond lattice. When using the true low-energy structure of boron [e.g., alpha-Boron or gamma- B_{28} (Ref. 13)] as the reference state in Eq. (2), the formation energies of all BC_5-m structures considered are positive, suggesting that they are all thermodynamically metastable structures in the B-C binary phase diagram. Such a conclusion is in agreement with the previous first-principles study of diamondlike BC_x structures by Lowther.¹⁴ It also explains why diamondlike BC_5 can only be prepared under extreme (high-pressure and high-temperature) conditions.

Interestingly, contrary to cubic BC_2N whose total energy is strongly structure dependent,^{15,16} we find that the total energies of BC_5-m structures are not very sensitive to lattice configuration (see Table I). Furthermore, with the exception of the BC_5-3 structure, the predicted “effective” cubic lattice parameters of BC_5-m structures are also very similar, all well within 1% of the experimentally measured value [$a = 3.635 \pm 0.006$ Å (Ref. 5)]. As a consequence, it is not possible to judge which structure is more likely only based on lattice parameter. Table I further shows the bond-type parameter, η , which has been adopted in the search for the most stable BC_2N structure.¹⁶ Here, η is defined as the fraction of nearest-neighbor B-B bonds relative to the total number of nearest-neighbor bonds, i.e.,

$$\eta = \frac{n_{B-B}}{n_{C-C} + n_{B-C} + n_{B-B}}, \quad (3)$$

where n denotes the number of a specific type of bond (i.e., B-B, C-C, and B-C) in the structure. Unlike BC_2N , we find no obvious correlation between the total energy of the structure and η , suggesting that there is no strong preference for specific type of chemical bonds.

Among the nine structures in Fig. 1, BC_5-2 is energetically the most favorable one with a negative formation energy, i.e., it is energetically stable with respect to phase separation into the pure constituents: diamond-B and diamond-C. The BC_5-2 structure can be viewed as a short period $(B_2)_1(C_2)_5$ superlattice structure formed by stacking one double layer of boron and five double layers of carbon along the $\langle 111 \rangle$ direction. Our calculations of the formation energies of several $(B_2)_N(C_2)_{5N}$ (111) superlattice structures ($N = 1, 2, \text{ and } 3$) confirm that the formation energy indeed increases (i.e., becomes less stable) and monotonically approaches zero with increasing N . Note that, this is in contrast to cubic BC_2N , which exhibits a tendency toward phase separation into pure zinc-blende BN and diamond-C.¹⁵⁻¹⁸

Besides the nine structures shown in Fig. 1, we have also considered all other pseudodiamond BC_5 structures with unit cells containing six and 12 atoms,^{15,19} resulting in additional 60 symmetrically inequivalent structures. Our calculations confirm that the BC_5-2 structure indeed has the lowest energy among all 69 possible structures, though our search has

TABLE I. Formation energy (ΔE) and equilibrium volume-per-atom (V) of different ordered and disordered BC_5 structures. The “effective” cubic lattice parameter of the diamond lattice is obtained as $a_{\text{cubic}} = 2\sqrt[3]{V}$. The bond-type parameter η (see text for definition) is also shown. The numbers shown in parentheses denote formation energies calculated using the CASTEP code.

Structure	BC_5-1	BC_5-2	BC_5-3	BC_5-4	BC_5-5	BC_5-6	BC_5-7	BC_5-8	BC_5-9	BC_5-10	BC_5-11	SQS-54
ΔE (eV/atom)	-0.015 (-0.020)	-0.064 (-0.070)	0.016 (-0.004)	-0.011 (-0.014)	-0.037 (-0.041)	-0.016 (-0.019)	-0.012 (-0.018)	-0.017 (-0.021)	-0.018 (-0.023)	-0.057 (-0.063)	-0.061 (-0.066)	-0.009 (-0.017)
V (Å ³ /atom)	6.015	5.993	6.667	6.020	6.021	6.016	6.016	6.014	6.013	6.037	6.016	6.043
a_{cubic} (Å)	3.637	3.633	3.764	3.638	3.638	3.637	3.637	3.637	3.637	3.642	3.637	3.643
η	0	0.125	0.042	0	0	0	0	0	0	0.083	0	0.028

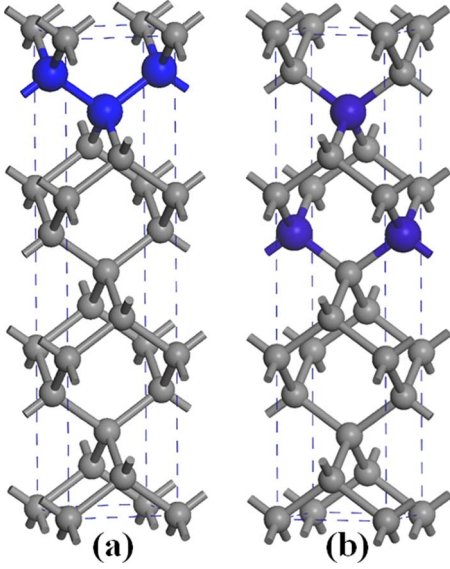


FIG. 2. (Color online) Crystal structures of (a) BC₅-10 and (b) BC₅-11 structures derived from the diamond lattice according to Eq. (4). The darker and lighter spheres indicate boron and carbon atoms, respectively.

also identified two other structures with formation energies very close to that of BC₅-2, hereinafter referred to as BC₅-10 [Fig. 2(a)] and BC₅-11 [Fig. 2(b)] structures. Both structures are based on the 12-atom tetragonal supercell with ideal c/a ratio of $3\sqrt{2}$, which can be derived from the eight-atom cubic diamond unit cell using the following transformation of lattice vector

$$\begin{pmatrix} 1 & 0 & 0 \\ 0 & 1 & 0 \\ 0 & 0 & 1 \end{pmatrix} \rightarrow \begin{pmatrix} 0.5 & -0.5 & 0 \\ 0.5 & 0.5 & 0 \\ 0 & 0 & 3 \end{pmatrix}. \quad (4)$$

Note that, to check the reliability of the results from VASP, we have also performed additional calculations using the CASTEP code²⁰ employing Vanderbilt-type ultrasoft pseudopotentials²¹ and GGA-PW91.²² In such calculations, the plane-wave cutoff energy is set at 450 eV and the Broyden-Fletcher-Goldfarb-Shanno minimization scheme²³ is used for geometry optimization. From Table I, it can be seen that the results from CASTEP also indicate BC₅-2 to be the lowest-energy structure.

In addition to the ordered structures discussed above, we have also generated a 54-atom special quasirandom structure (SQS) (Refs. 24–26) to mimic the fully disordered state of

TABLE III. Structural description of the SQS-54 structure (space group $P1$) for the random diamondlike BC₅. Lattice vectors and atomic positions are given in Cartesian coordinates, in units of a , the lattice parameter of the cubic diamond unit cell. Atomic positions are given for the ideal, unrelaxed diamond sites.

Lattice vectors: $a_1=(0, 1.5, 1.5)$, $a_2=(1.5, 0, 1.5)$, $a_3=(1.5, 1.5, 0)$		
Atomic positions of carbon (x, y, z)		
(1.0, 1.0, 0.0)	(1.5, 0.5, 1.0)	(2.0, 1.0, 1.0)
(0.0, 0.5, 0.5)	(1.0, 1.5, 0.5)	(0.5, 0.5, 1.0)
(1.0, 1.0, 1.0)	(1.0, 0.5, 1.5)	(1.5, 1.0, 1.5)
(0.0, 1.0, 1.0)	(0.5, 1.5, 1.0)	(1.0, 2.0, 1.0)
(1.0, 1.5, 1.5)	(1.5, 2.0, 1.5)	(1.0, 1.0, 2.0)
(2.0, 2.0, 2.0)	(0.75, 0.75, 0.25)	(1.75, 1.25, 0.75)
(1.75, 0.75, 1.25)	(0.25, 0.75, 0.75)	(1.25, 1.75, 0.75)
(0.75, 0.75, 1.25)	(1.75, 1.75, 1.25)	(1.75, 1.25, 1.75)
(2.25, 1.75, 1.75)	(0.75, 1.75, 1.25)	(1.25, 2.25, 1.25)
(0.75, 1.25, 1.75)	(1.75, 2.25, 1.75)	(1.25, 1.25, 2.25)
(1.75, 1.75, 2.25)	(2.25, 2.25, 2.25)	(1.0, 0.0, 1.0)
(2.0, 1.5, 1.5)	(1.25, 0.75, 0.75)	(0.75, 1.25, 0.75)
(1.25, 1.25, 1.25)	(1.25, 0.75, 1.75)	(0.5, 0.5, 0.0)
(0.5, 1.0, 1.5)	(0.25, 0.25, 0.25)	(1.25, 1.25, 0.25)
(1.25, 0.25, 1.25)	(1.5, 1.5, 2.0)	(1.25, 1.75, 1.75)
Atomic positions of boron (x, y, z)		
(0.0, 0.0, 0.0)	(0.5, 0.0, 0.5)	(1.0, 0.5, 0.5)
(1.5, 1.0, 0.5)	(0.5, 1.0, 0.5)	(1.5, 1.5, 1.0)
(2.25, 1.25, 1.25)	(0.75, 0.25, 0.75)	(0.25, 1.25, 1.25)

diamondlike BC₅, in which boron atoms are randomly distributed on the diamond lattice. The key idea of the SQS approach is to adequately reproduce the statistics of a random alloy in a relatively small and thus computationally feasible supercell. Furthermore, due to the atomistic nature of the SQS approach, effects such as local atomic relaxation and charge transfer can be fully considered. As shown in Table II, the pair and three-body correlation functions of our generated SQS-54 structure are in excellent agreement with those of the random diamond alloy. Detailed structural information of the SQS-54 structure is given in Table III. Crystal structure of BC₅, in its ideal and unrelaxed form, is also shown in Fig. 3. Importantly, we find only a small energy difference of 0.055 eV/atom between the fully disordered SQS-54 structure and the energetically most favorable ordered BC₅-2 structure, indicating that there is only a weak

TABLE II. Pair and multisite correlation functions of 54-atom SQS structure for mimicking random diamond-type BC₅. $\bar{\Pi}_{k,m}$ denotes the correlation function of figure $f=(k,m)$ that has k vertices and spans a maximum distance of m ($m=1,2,3,\dots$ are the first-, second-, third-nearest neighbors, etc.) For the perfectly random B_xC_{1-x}, $\bar{\Pi}_{k,m}=(2x-1)^k$ since there is no correlation in the occupation between various sites.

Figure	$\bar{\Pi}_{2,1}$	$\bar{\Pi}_{2,2}$	$\bar{\Pi}_{2,3}$	$\bar{\Pi}_{2,4}$	$\bar{\Pi}_{2,5}$	$\bar{\Pi}_{3,2}$	$\bar{\Pi}_{3,2}$	$\bar{\Pi}_{3,2}$	$\bar{\Pi}_{3,3}$	$\bar{\Pi}_{3,3}$	$\bar{\Pi}_{3,3}$
SQS-54	0.444	0.444	0.444	0.432	0.432	-0.309	-0.296	-0.296	-0.302	-0.284	-0.321
Random	0.444	0.444	0.444	0.444	0.444	-0.296	-0.296	-0.296	-0.296	-0.296	-0.296

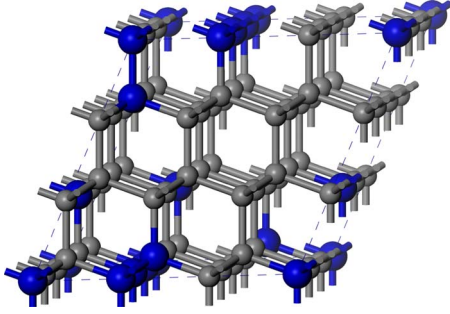


FIG. 3. (Color online) Illustration of the crystal structure for BC_5 with boron randomly distributed on the diamond lattice (SQS-54). The darker and lighter spheres denote boron and carbon atoms, respectively.

ordering tendency of BC_5 . From the energy difference between the ordered and disordered state and assuming ideal configurational entropy of mixing for the disordered diamond BC_5 alloy, we can further estimate the order-disorder temperature of BC_5 using the following equation

$$T_c \approx -\frac{E_{disordered} - E_{ordered}}{k_B[x \ln x + (1-x)\ln(1-x)]}, \quad (5)$$

where $x=1/6$ for BC_5 and k_B is the Boltzmann constant. From Eq. (5), we obtain $T_c \approx 1397$ K. The predicted order-disorder temperature is well below the experimental synthesizing temperature of 2200 K,⁵ which suggests that the diamondlike BC_5 phase synthesized under experimental conditions is likely to be disordered assuming a sluggish kinetics during the recovery process.

In order to substantiate this conclusion, we have directly obtained the bulk moduli of ordered and disordered BC_5 structures by fitting first-principles calculated total energies at different volumes to an integrated third-order Birch-Murnaghan equation of state (EOS).²⁷ At each volume, the unit cell shape and all internal atomic coordinates are fully relaxed. The predicted pressure-volume relationships of BC_5 -1, BC_5 -2, and SQS-54 are displayed in Fig. 4. The EOS

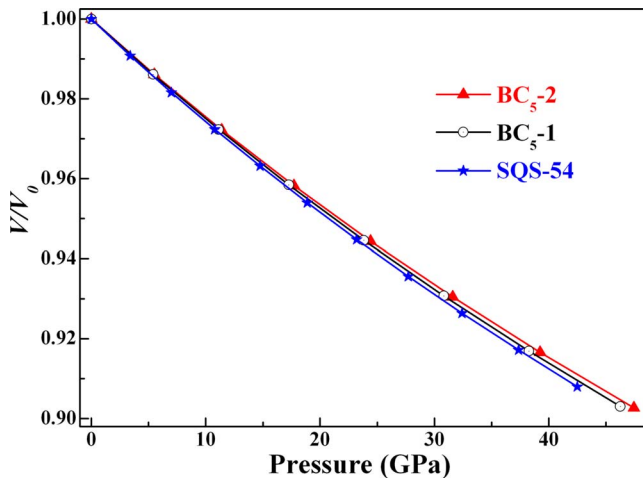


FIG. 4. (Color online) Pressure dependence of unit cell volume for BC_5 with BC_5 -1, BC_5 -2, and SQS-54 structures.

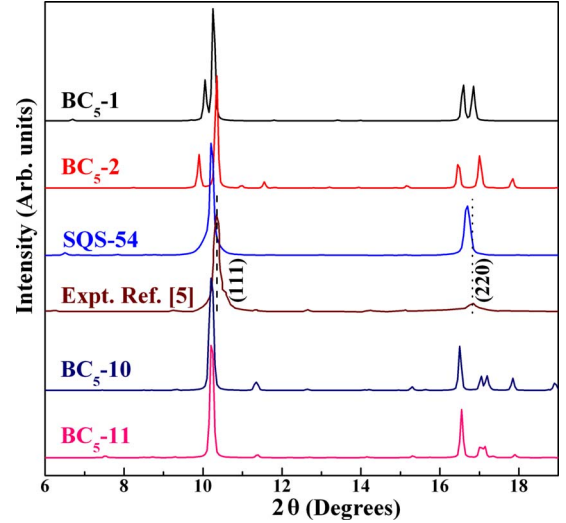


FIG. 5. (Color online) Calculated x-ray diffraction patterns for BC_5 -1, BC_5 -2, BC_5 -10, BC_5 -11, and SQS-54 structures at ambient conditions ($\lambda=0.3738$ Å). The experimental profile at 24 GPa and 2200 K from Ref. 5 is also included.

data for BC_5 -10 and BC_5 -11 are very similar to those of BC_5 -1, and thus not shown for brevity. Compared with the ordered candidate structures (the EOS fitted bulk moduli for BC_5 -1, BC_5 -2, BC_5 -10, and BC_5 -11 are 376, 385, 375, and 378 GPa, respectively), the fitted bulk modulus of the SQS-54 structure (366 GPa) is in better agreement with the experimental value [$B_0=335 \pm 8$ GPa (Ref. 5)]. Furthermore, the pressure derivative of bulk modulus of SQS-54 (3.81) is also in better agreement with experiment [$B'_0=4.5 \pm 0.6$ (Ref. 5)] than those of the four ordered ones (3.62–3.65).

As a more stringent test, we have simulated the powder XRD patterns of BC_5 -1, BC_5 -2, BC_5 -10, BC_5 -11, and SQS-54 structures. Such simulations have now been widely used in the literature to aid the identification of unknown crystal structures.^{28–30} The calculated XRD results ($\lambda=0.3738$ Å) are shown in Fig. 5 in comparison with experimental data. Again, the disordered structural model gives XRD pattern in best agreement with experiments. For BC_5 - m ($m=1, 2, 10, 11$) ordered structures, the 111 and/or 220 peaks exhibit large difference from the experimental data due to the presence of peak splitting. Note that such a conclusion is in accordance with a recent study by Yao *et al.*⁷ Finally, it is worth pointing out that the shifts of peaks between the pattern for SQS-54 and the experimental one can be attributed to the different temperature and pressure conditions: experimental pattern was taken at 24 GPa and 2200 K while our simulated profile corresponds to ambient pressure and temperature conditions. In addition, we estimate the coefficient of thermal expansion at 24 GPa based on the calculated EOS data (Fig. 4) and the experimental x-ray diffraction pattern. The average volumetric and linear (calculated using effective cubic lattice constant a_{cubic}) thermal expansion coefficients for BC_5 at 24 GPa in the temperature range of 300–2200 K are $\alpha_V=8.6 \times 10^{-6}$ K⁻¹ and $\alpha_L=2.9 \times 10^{-6}$ K⁻¹, respectively. These values are in excellent consistent with those reported by Xie *et al.*³¹ They calculated the coefficient of

TABLE IV. First-principles calculated single-crystal elastic constants c_{ij} (GPa) of the ordered BC₅-2 structure and the random BC₅ structure. The cubic elastic constants of the latter are obtained by averaging the c_{ij} 's of the low-symmetry SQS-54 structure. Polycrystalline bulk modulus B (GPa), shear modulus G (GPa), Young's moduli E (GPa), and Poisson's ratio ν are calculated using the Hill's approximation. The predicted elastic properties of the ordered BC₅-1 structure as adopted by Calandra and Mauri (Ref. 6) are also included.

Structure	c_{11}	c_{33}	c_{12}	c_{13}	c_{14}	c_{44}	B	G	E	ν	B_{EOS}	B'_0
BC ₅ -1	832	1006	181	90	-101	368	377	351	803	0.15	376	3.65
BC ₅ -2	930	1034	115	85	-68	389	385	405	900	0.11	385	3.63
Random	708		196			426	367	347	792	0.14	366	3.81

thermal expansion of diamond under various pressures; the obtained α_l for diamond under 20 GPa in the 100–1600 K is in the range of $0-4.2 \times 10^{-6} \text{ K}^{-1}$.

Finally, to check the mechanical stability of the ordered BC₅-2 structure as well as the disordered BC₅ structure, we have calculated their independent single-crystal elastic constants using an efficient strain-stress method,³² i.e., through a linear least-squares fit of first-principles calculated stress as a function of imposed strain. At each given strain, we fully relax all internal atomic coordinates according to strain-induced forces while holding the distorted lattice vectors fixed. From Table IV, it can be seen that both structures are mechanically stable since their elastic constants obey the elastic stability criteria, i.e., the strain energy must be positive against any homogeneous elastic deformation.³³ From the calculated c_{ij} 's, we further estimate the polycrystalline bulk modulus B and shear modulus G using the Voigt-Reuss-Hill approximation.³⁴ As shown in Table IV, the bulk moduli calculated from second-order elastic constants are in very good agreement with the EOS fitted values, which further confirms the reliability of the present calculations. According to Teter,³⁵ the polycrystalline shear modulus is a better pre-

dictor of hardness than bulk modulus. Table IV shows that diamondlike BC₅ structures exhibit very large shear moduli comparable to that of diamond, which explains its high hardness as was observed experimentally.

In summary, using first-principles density-functional calculations, we investigate the possible crystal structures of the superhard diamondlike BC₅. Interestingly, our systematic search for the energetically most favorable configuration indicates that BC₅ exhibits only a weak tendency toward ordering. As a consequence, the BC₅ compound synthesized experimentally at high temperatures is likely to be disordered. In other words, boron atoms are distributed randomly on the underlying diamond lattice. Such a conclusion is further supported by the evidence that the disordered state gives bulk modulus and x-ray diffraction pattern in good agreements with experimentally reported data.

All calculations are performed using the parallel computing facilities at Los Alamos National Laboratory (LANL). This research is supported by LANL, which is operated by Los Alamos National Security LLC under DOE under Contract No. DEAC52-06NA25396.

*Corresponding author.

†chao@lanl.gov

‡zlin@lanl.gov

§yzhao@lanl.gov

¹M. L. Cohen, Phys. Rev. B **32**, 7988 (1985).

²V. L. Solozhenko, D. Andrault, G. Fiquet, M. Mezouar, and D. C. Rubie, Appl. Phys. Lett. **78**, 1385 (2001).

³Y. Zhao, D. He, L. Daemen, T. Shen, R. Schwarz, Y. Zhu, D. Bish, J. Huang, J. Zhang, G. Shen, J. Qian, and W. Zerda, J. Mater. Res. **17**, 3139 (2002).

⁴V. L. Solozhenko, N. A. Dubrovinskaia, and L. S. Dubrovinsky, Appl. Phys. Lett. **85**, 1508 (2004).

⁵V. L. Solozhenko, O. O. Kurakevych, D. Andrault, Y. L. Godec, and M. Mezouar, Phys. Rev. Lett. **102**, 015506 (2009).

⁶M. Calandra and F. Mauri, Phys. Rev. Lett. **101**, 016401 (2008).

⁷Y. Yao, J. S. Tse, and D. D. Klug, Phys. Rev. B **80**, 094106 (2009).

⁸Y. C. Liang, W. Q. Zhang, J. Z. Zhao, and L. F. Chen, Phys. Rev. B **80**, 113401 (2009).

⁹J. P. Perdew, K. Burke, and M. Ernzerhof, Phys. Rev. Lett. **77**, 3865 (1996).

¹⁰G. Kresse and J. Furthmüller, Phys. Rev. B **54**, 11169 (1996).

¹¹C. Jiang, Z. J. Lin, J. Z. Zhang, and Y. S. Zhao, Appl. Phys. Lett. **94**, 191906 (2009).

¹²H. J. Monkhorst and J. D. Pack, Phys. Rev. B **13**, 5188 (1976).

¹³A. R. Oganov, J. H. Chen, C. Gatti, Y. Z. Ma, Y. M. Ma, C. W. Glass, Z. X. Liu, T. Yu, O. O. Kurakevych, and V. L. Solozhenko, Nature (London) **457**, 863 (2009).

¹⁴J. E. Lowther, J. Phys.: Condens. Matter **17**, 3221 (2005).

¹⁵S. Y. Chen, X. G. Gong, and S. H. Wei, Phys. Rev. Lett. **98**, 015502 (2007).

¹⁶S. Y. Chen, X. G. Gong, and S. H. Wei, Phys. Rev. B **77**, 014113 (2008).

¹⁷R. Q. Zhang, K. S. Chan, H. F. Cheung, and S. T. Lee, Appl. Phys. Lett. **75**, 2259 (1999).

¹⁸E. Kim, T. Pang, W. Utsumi, V. L. Solozhenko, and Y. S. Zhao, Phys. Rev. B **75**, 184115 (2007).

¹⁹L. G. Ferreira, S. H. Wei, and A. Zunger, Int. J. Supercomput. Appl. **5**, 34 (1991).

²⁰M. D. Segall, P. L. D. Lindan, M. J. Probert, C. J. Pickard, P. J. Hasnip, S. J. Clark, and M. C. Payne, J. Phys.: Condens. Matter **14**, 2717 (2002).

- ²¹D. Vanderbilt, Phys. Rev. B **41**, 7892 (1990).
- ²²J. P. Perdew, J. A. Chevary, S. H. Vosko, K. A. Jackson, M. R. Pederson, D. J. Singh, and C. Fiolhais, Phys. Rev. B **46**, 6671 (1992).
- ²³B. G. Pfrommer, M. Côté, S. G. Louie, and M. L. Cohen, J. Comput. Phys. **131**, 233 (1997).
- ²⁴A. Zunger, S. H. Wei, L. G. Ferreira, and J. E. Bernard, Phys. Rev. Lett. **65**, 353 (1990).
- ²⁵S. H. Wei, L. G. Ferreira, J. E. Bernard, and A. Zunger, Phys. Rev. B **42**, 9622 (1990).
- ²⁶C. Jiang, C. Wolverton, J. Sofo, L. Q. Chen, and Z. K. Liu, Phys. Rev. B **69**, 214202 (2004).
- ²⁷F. Birch, J. Geophys. Res. **83**, 1257 (1978).
- ²⁸Q. Li, M. Wang, A. R. Oganov, T. Cui, Y. M. Ma, and G. T. Zou, J. Appl. Phys. **105**, 053514 (2009).
- ²⁹Q. Li, Y. M. Ma, A. R. Oganov, H. B. Wang, H. Wang, Y. Xu, T. Cui, H. K. Mao, and G. T. Zou, Phys. Rev. Lett. **102**, 175506 (2009).
- ³⁰X. F. Zhou, J. Sun, Q. R. Qian, X. Guo, and Z. Y. Liu, J. Appl. Phys. **105**, 093521 (2009).
- ³¹J. J. Xie, S. P. Chen, J. S. Tse, S. D. Grioncoli, and S. Baroni, Phys. Rev. B **60**, 9444 (1999).
- ³²C. Jiang, Appl. Phys. Lett. **92**, 041909 (2008).
- ³³J. F. Nye, *Physical Properties of Crystals* (Oxford University Press, Oxford, 1985).
- ³⁴R. Hill, Proc. Phys. Soc. London **65**, 350 (1952).
- ³⁵D. M. Teter, MRS Bull. **23**, 22 (1998).